Conformational preferences of heteronuclear Fischer carbene complexes of cymantrene and cyclopentadienyl rhenium tricarbonyl

*Roan Fraser, Petrus H. van Rooyen and Marilé Landman**

Department of Chemistry, University of Pretoria, Private Bag X20, Hatfield, 0028, South Africa. Tel: +27-12-4202527, Fax: +27-12-4204687

Contact author details:
Name: Marilé Landman Tel: +27-12-4202527, Fax: +27-12-4204687, email: marile.landman@up.ac.za

Keywords

Fischer carbene; cymantrenyl; cyclopentadienyl rhenium tricarbonyl; DFT; NBO analysis

Graphical abstract

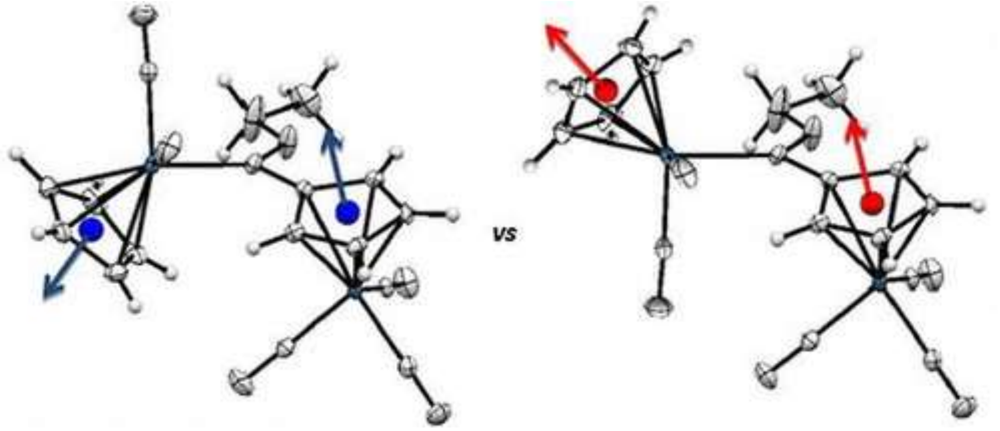

TOC abstract

Synthesis, single crystal X-ray study and NBO analysis of Fischer ethoxy carbene complexes with cymantrenyl and cyclopentadienyl rhenium tricarbonyl substituents

Research highlights

- DFT calculations on configurations of homo- and heteronuclear complexes
- Crystal structure of first carbene complex containing a mixed cyclopentadienyl rhenium tricarbonyl and cymantrene system
- Calculated energy diagram for the synthetic methodology of the *trans* carbene complexes

- Calculated energy values, comparing the *cis* and *trans* carbene formation

Abstract

Homo- and heteronuclear bimetallic carbene complexes of group VII transition metals (Mn and Re), with cymantrene or cyclopentadienyl rhenium tricarbonyl as the starting synthon, have been synthesised according to classic Fischer methodology. Crystal structures of the novel carbene complexes with general formula $[RC_5H_4M'(CO)_2\{C(OEt)(C_5H_4M(CO)_3)\}]$, where M = M' = Mn, R = H (**1**), R = Me (**2**); M = Mn, M' = Re, R = H (**3**); M = M' = Re, R = H (**4**) and M = Re, M' = Mn, R = H (**5**) are reported. A density functional theory (DFT) study was undertaken to determine natural bonding orbitals (NBOs) and conformational as well as isomeric aspects of the binuclear complexes. Application of the second-order perturbation theory (SOPT) of the NBO method revealed stabilizing interactions between the methylene C-H bonds and the carbonyl ligands of the carbene metal moiety. Energy calculations in the gas phase of the *cis* and *trans* conformations of the Cp rings relative to one another are comparable, with the *trans* conformation slightly lower in energy. The theoretical findings have also been confirmed with single crystal X-ray diffraction and all solid state structures are found in the *trans* geometry.

1 Introduction

Metal carbene complexes as discovered by E.O Fischer in the 1960's, have since been established as irreplaceable building blocks for the synthesis of organic molecules [1,2]. Fischer carbene complexes have found application in cycloaddition reactions [3], heterocyclization [4], catalytic carbene transfer reactions [5] and in the so-called Dötz benzannulation reactions [6]. The synthesis of Fischer carbene complexes from metal-containing carbene substituents are well described in literature. Carbene complexes of ruthenocene [7], ferrocene [8] and cyclopentadienyl metal half sandwich moieties [9] are known and the electrochemical properties of these complexes examined [9] (Figure 1).

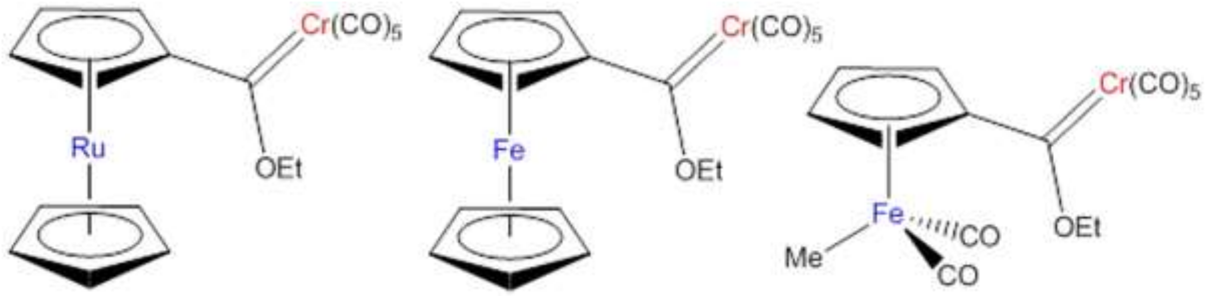

Figure 1: Multi-metal carbene complexes containing a Cp metal bearing moiety

A study on the synthesis and structural aspects of multi-metal carbene complexes, bearing cymantrene as the carbene substituent, was recently published by our research group [10]. This study found NBO stabilizing interactions between the C-H atoms of the cyclopentadienyl of the cymantrenyl substituent and the carbene metal carbonyl ligands (Figure 2).

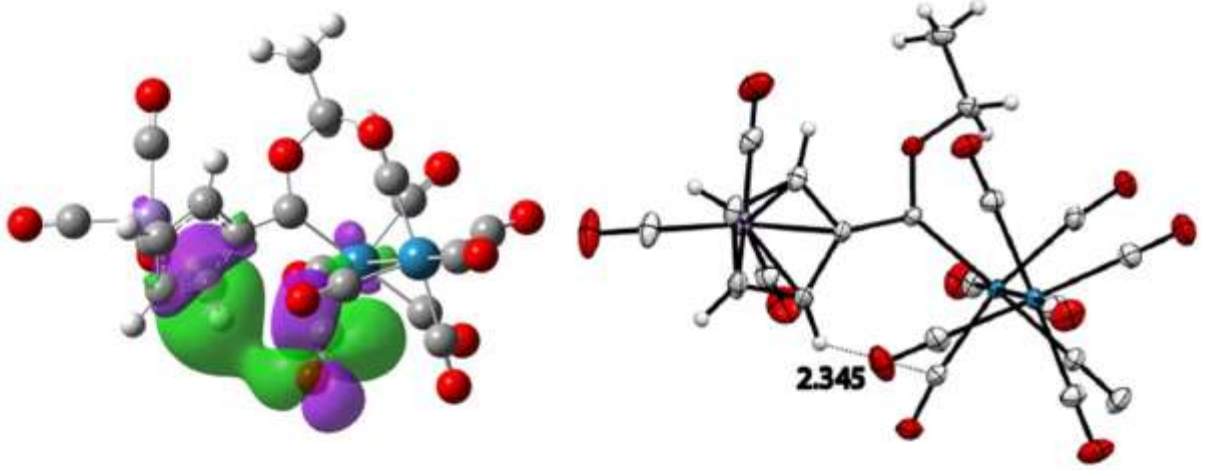

Figure 2: NBO interaction between the cyclopentadienyl C-H atoms and the carbene metal carbonyl ligands of the cymantrenyl dirhenium carbene complex

The study also indicated additional NBO stabilization interactions between the methylene protons and the carbonyl ligands situated on the carbene metal moiety. A linear decrease in NBO stabilizing interactions was observed down the group, for the group VI metal carbene complexes (Cr > Mo > W). The total second-order perturbation theory (SOPT) energy thus decreases in the order Cr > Mo > W [10].

Incidences of non-covalent intramolecular interligand interactions were also described by Lugan and Lavigne [11] when methylene protons of methoxycarbene complexes interacted with carbonyls associated with the carbene moiety. These interactions were determined using

NBO calculations and indicated additional intramolecular stabilizations supporting the conformational aspects found in the solid state structure. The finding also supports seminal MO calculations by Hoffmann *et al*. [12] that predicted that carbene ligands in piano-stool complexes preferred the so-called vertical coordination mode rather than the horizontal mode (Figure 3).

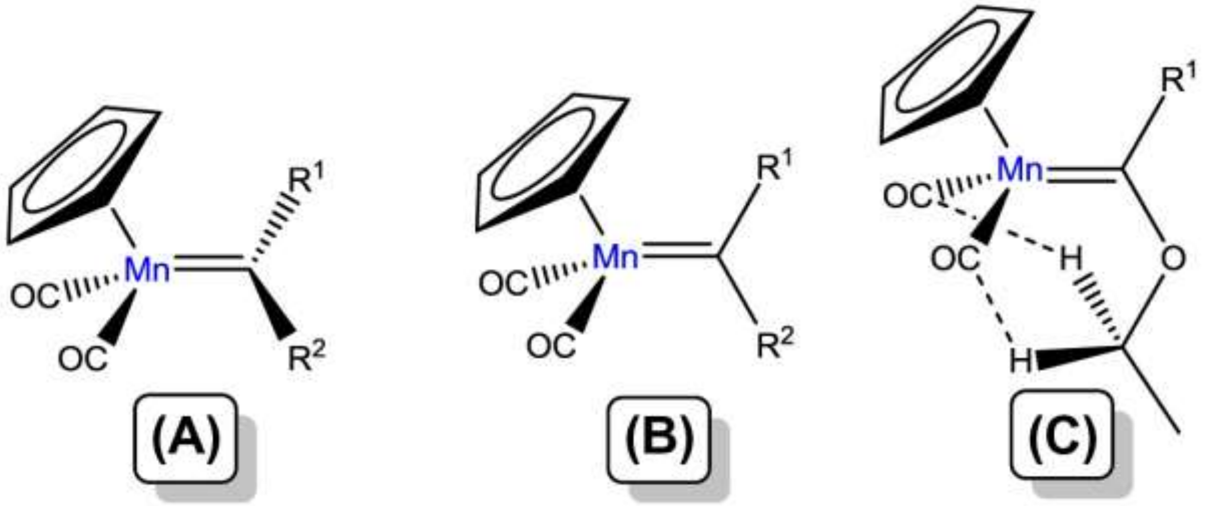

Figure 3: The horizontal coordination mode (A), the vertical coordination mode (B) and the stabilization of the vertical coordination mode (C) as described by Lugan and Lavigne

Complexes where $MnCp(CO)_3$ and $ReCp(CO)_3$ constitute both the initial building synthons as well as the metallating agent have been studied and published by Fischer [13] and Casey [14] (Figure 4). Their studies are restricted to either homonuclear carbene complexes or carbene complexes of group VI and according to our knowledge constitute the only other examples where the cymantrene and cyclopentadienyl rhenium substituents serve as both the initial deprotonated moiety and metallating agent.

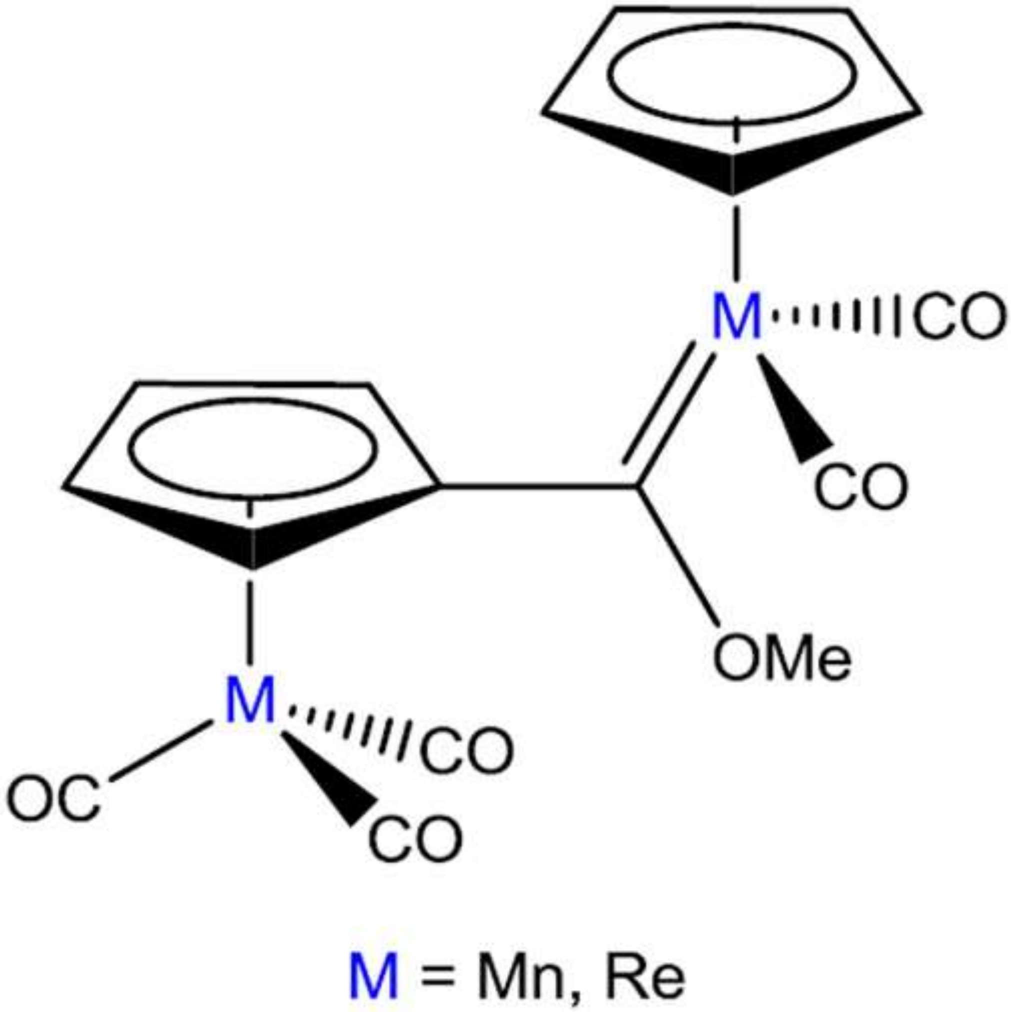

Figure 4: Homonuclear carbene complexes containing $MCp(CO)_3$ (M = Mn, Re) as initial building blocks synthesised by Fischer [13] and Casey [14]

The abovementioned carbene complexes may present either a *cis* or *trans* conformation of the cyclopentadienyl ring of the cymantrenyl substituent relative to the carbene metal moiety (Figure 5). Theoretical calculations on the homonuclear carbene complexes indicate similar energies between the two conformers with the *trans* conformation lower in energy by only 1.2 kJ/mol. Several intermolecular close contact interactions in the packing of this molecule are observed supporting the formation of the *trans*-conformation [10].

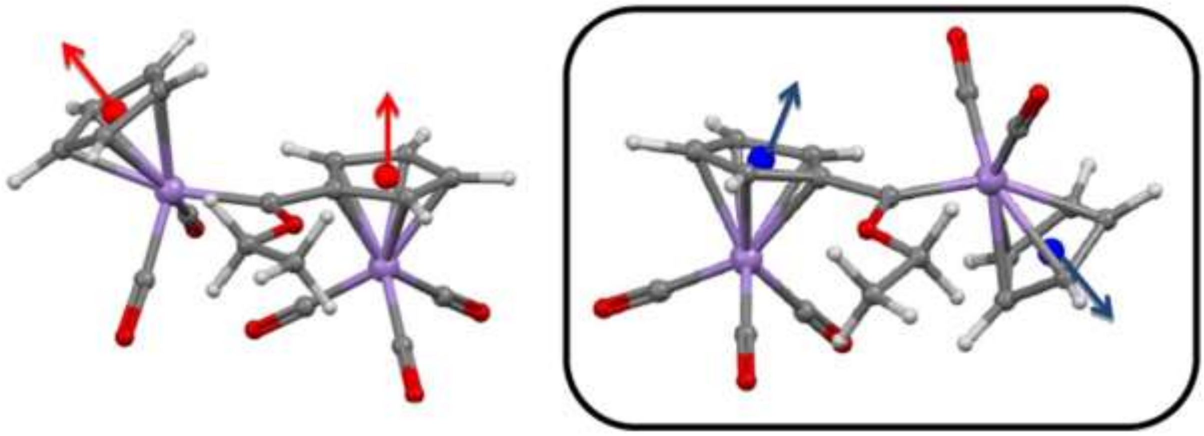

Figure 5: Optimized *cis* (left) and *trans* (right) conformations for the homonuclear cymantrenyl carbene complex

Based on these existing studies, a DFT study was initiated to extend the scope and understanding of multi-metallic systems focussing on homo- and heteronuclear carbene complexes bearing cymantrenyl and cyclopentadienyl rhenium tricarbonyl substituents. This study reports the synthesis of the four novel homo- and heteronuclear bimetallic complexes of group VII transition metals (Figure 6), crystal structures of three of the complexes and a DFT study.

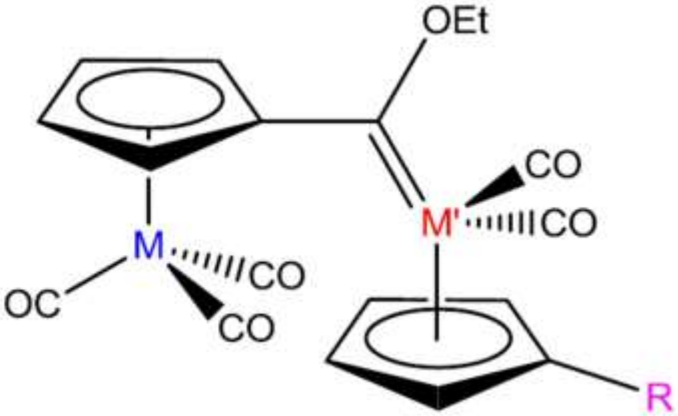

1 M = Mn, M' = Mn, R = H
2 M = Mn, M' = Mn, R = Me
3 M = Mn, M' = Re, R = H
4 M = Re, M' = Re, R = H
5 M = Re, M' = Mn, R = H

Figure 6: Bimetallic monocarbene complex 1-5

2 Experimental

2.1 Materials and instrumentation

All reactions, unless otherwise noted, were performed under inert nitrogen or argon atmospheres using standard Schlenk techniques [15]. All solvents were freshly distilled, dried and collected under inert conditions. Column chromatography was carried out under inert nitrogen and argon atmospheres using silica gel (particle size 0.063-0.200 mm) as the stationary phase. Percentage yields were calculated relative to the limiting reactant. Crystallization was done using hexane:DCM or hexane:ether diffusion methods. Triethyloxonium tetrafluoroborate [16] was prepared according to a reported literature procedure. The reagents $CpMn(CO)_3$, $MeCpMn(CO)_3$, $CpRe(CO)_3$, n-butyl lithium (1.6 M solution in hexane) and other commercial reagents were used as purchased. NMR spectra were recorded on a Bruker ARX-300. NMR spectra were recorded in CDCl3 using the deuterated solvent peak as internal reference. ^1H and ^{13}C NMR spectra were measured at 300.1 and 75.5 MHz, respectively. The numbering of atoms in the NMR assignment is according to the numbers used Figure 7 - Figure 9. IR spectra were recorded on a Perkin Elmer Spectrum RXI FT-IR spectrophotometer as KBr pellets and only the vibration bands in the carbonyl-stretching region (ca. 1500-2200 cm^{-1}) are reported.

2.2 X-ray crystallography

Data for complexes **2** and **4** and **5** were collected at 150 K on a Bruker D8 Venture kappa geometry diffractometer, with duo Iμs sources, a Photon 100 CMOS detector and APEX II control software using Quazar multi-layer optics, monochromated Mo-Kα radiation and by means of a combination of ϕ and ω scans. Data reduction was performed using SAINT+ and the intensities were corrected for absorption using SADABS [17]. The structures were solved by intrinsic phasing using SHELXTS and refined by full-matrix least squares using SHELXTL and SHELXL-2013 [18]. In the structure refinement, all hydrogen atoms were added in calculated positions and treated as riding on the atom to which they are attached. All nonhydrogen atoms were refined with anisotropic displacement parameters, all isotropic displacement parameters for hydrogen atoms were calculated as X × Ueq of the atom to which they are attached, X = 1.5 for the methyl hydrogens and 1.2 for all other hydrogens. Crystallographic data and refinement parameters are given in Table 1. Ortep drawings [19] of the three structures are included in Figure 7, Figure 8 and Figure 9. In the structure of **5**, some metal mixing occurs, where both metals Mn and Re are present at both metal positions (6% mixing). However, the major component of this structure is the complex where the substituent metal atom is Re and the carbene metal atom is Mn, *i.e.* **5** (94%). The crystal structures (cif) have been deposited at the Cambridge Crystallographic Data Centre and allocated the deposition numbers: CCDC 1482771-1482773. Data collection, structure solution and refinement details are available in each cif.\

2.3 Synthesis of complexes 1-5

2.3.1 Synthesis of 1

Complex **1** has been synthesised and reported previously [10].

2.3.2 Synthesis of 2

$CpMn(CO)_3$ (0.612 g, 3.0 mmole) was dissolved in 40 ml of dry THF. n-Butyl lithium (2.00 ml, 3.0 mmole) was added at -30 ˚C and stirred at this temperature for 30 min. The colour of the reaction mixture changed from yellow to a dark brown colour. $MeCpMn(CO)_3$ (0.654 g, 3.0 mmole) were added to the reaction mixture at -79˚C and allowed to react at this temperature for 1 hour and warmed to room temperature. After completion of the reaction, the solvent was removed *in vacuo* and the residue redissolved in dichloromethane. Triethyl oxonium tetrafluoroborate (0.55 g, 3.0 mmole) was dissolved in 20 ml of dichloromethane and this was added to the cooled reaction mixture (-20˚C). An immediate colour change was observed, from brown to a deep red solution, and the reaction mixture was dry loaded onto a silica gel column for purification. The product was isolated using a 10:1 hexane: DCM eluent ratio. A single brown product was isolated of complex **2** (yield: 0.720g; 50%)^{1}H NMR (300 MHz, $CDCl_3$): δ = 5.51 (s, 2H, H_{17} and H_{14}); 4.93 (s, 2H, H_{15} and H_{16}); 5.12 (q, 2H, J_{HH} = 7.1, O**CH₂**CH₃); 1.65 (t, 3H, J_{HH} = 6.7, $OCH_2\mathbf{CH_3}$). $^{13}C\{^1H\}$ NMR (75.5 MHz, $CDCl_3$): $C_{(Carbene)}$ 331.0; $Mn(\mathbf{CO})_3$ 222.8; MeMn(**CO**) 222.6; C_5H_4 106.6; C_5H_4 87.6; C_5H_4 83.8; $O\mathbf{CH_2}CH_3$ 77.2; $OCH_2\mathbf{CH_3}$ 15.1**.** IR (cm^{-1}): 2064 (s), 2031 (s), 1946 (s), 1922 (m). HRESI$^+$-MS, m/z: 450.9779 (calcd 450.9786).

2.3.3 Synthesis of 3

The syntheses of **3**-**5** were done using a similar procedure as for the synthesis of **2**. $CpMn(CO)_3$ (0.612 g, 3.0 mmole) was dissolved in THF and lithiated at -30 ˚C. The lithiated Cp metal moiety was then metallated with 1.062 g (3.00 mmole) of $CpRe(CO)_3$ and quenched with the oxonium salt. A single brown product was isolated: a dark brown monocarbene complex **3** (yield: 0.766 g; 45%). ^{1}H NMR (300 MHz, $CDCl_3$): δ = 5.58 (s br, 5H, C_5H_5), 5.50 (s br, 2H, C_5H_4); 5.00 (s br, 2H, C_5H_4); 4.68 (s br, 2H, $O\mathbf{CH_2}CH_3$); 1.51 (s br, 3H, $OCH_2\mathbf{CH_3}$). $^{13}C\{^1H\}$ NMR (75.5 MHz, $CDCl_3$): $C_{(Carbene)}$ 273.8; CpMn(CO) 223.5; CpRe(CO) 206.5; C_5H_4 (ipso) 113.9; C_5H_4 89.4; C_5H_4 88.8; C_5H_5 85.0; $O\mathbf{CH_2}CH_3$ 74.3; $OCH_2\mathbf{CH_3}$ 14.3. IR (cm^{-1}): 2028 (m), 1952 (m), 1940 (s), 1896 (m). HRESI$^+$-MS, m/z: 568.9846 (calcd 568.9806).

2.3.4 Synthesis of 4

A 0.671g (2.0 mmole) of $CpRe(CO)_3$ was dissolved in THF and lithiated at -30 ˚C. The lithiated Cp moiety was then metallated with a second equivalent of $CpRe(CO)_3$ (0.671, 2.0 mmole) and quenched with the oxonium salt. One product was isolated: a red monocarbene complex 4 (yield: 0.699g; 50%).^{1}H NMR (300 MHz, $CDCl_3$): $\delta = 5.82$ (s, 2H, C_5H_4); 5.37 (s, 5H, C_5H_5); 5.29 (s, 2H, C_5H_4); 4.51 (q, 2H, $J_{HH} = 7.1$, $O\mathbf{CH_2}CH_3$); 1.55 (t, 3H, $J_{HH} = 7.0$, $OCH_2\mathbf{CH_3}$). $^{13}C\{^1H\}$ NMR (75.5 MHz, $CDCl_3$): $C_{(Carbene)}$ 269.1; Re(CO) 202.3; Re(CO) 193.8; C_5H_4 (ipso) 87.4; C_5H_5 86.2; C_5H_4 84.5; C_5H_4 82.8; $O\mathbf{CH_2}CH_3$ 74.9; $OCH_2\mathbf{CH_3}$ 14.4. IR (cm^{-1}): 2030 (m), 1969 (m), 1941 (s), 1889 (m). HRESI$^+$-MS, m/z: 700.9908 (calcd 700.9983).

2.3.4 Synthesis of 5

A 0.671g (2.0 mmole) of $CpRe(CO)_3$ was dissolved in THF and lithiated at -30 ˚C. The lithiated Cp moiety was then metallated with a second equivalent of $CpMn(CO)_3$ (0.436, 2.0 mmole) and quenched with the oxonium salt. One product was isolated: a brown monocarbene complex **5** (yield: 0.522g; 46%) ^{1}H NMR (300 MHz, $CDCl_3$): 5.31(s, 2H, C_5H_4); 5.08(s, 2H, C_5H_4); 4.65 (s, 5H, C_5H_5); 4.54(q, 2H, $J_{HH} = 7.4$, $O\mathbf{CH_2}CH_3$); 1.31(t, 3H, $J_{HH} = 7.0$, $OCH_2\mathbf{CH_3}$). $^{13}C\{^1H\}$ NMR (75.5 MHz, $CDCl_3$): $C_{(Carbene)}$ 331.3; Mn(CO) 230.8; Re(CO) 193.5; C_5H_4 (ipso) 94.2; C_5H_4 86.8; C_5H_5 83.8; C_5H_4 83.4; $O\mathbf{CH_2}CH_3$ 73.1; $OCH_2\mathbf{CH_3}$ 14.5. IR (cm^{-1}): 2028 (m), 1952 (s), 1939 (s), 1896 (m). HRESI$^+$-MS, m/z: 568.9846 (calcd 568.9806).

2.4 Molecular modelling

The calculations reported in this paper were obtained using the Gaussian 09 [20] suite of programs. Calculations were carried out in the singlet spin state using the hybrid functional B3LYP [21,22]. Geometries of the neutral complexes were optimized in gas phase with the triple-ζ basis set 6-311G* on all atoms except for the metal atoms. Stuttgart/Dresden (SDD) pseudopotential was used to describe the metal electronic core, while the valence electrons were described using def2-TZVPP [23]. No symmetry constraints were applied and only the default convergence criteria were used during the geometric optimizations. Vibrational frequencies [24] were calculated at the optimized geometries and no imaginary frequencies were observed, to confirm true minima. Donor-acceptor interactions have been computed using the natural bonding orbital (NBO) method [25].

3 Results and discussion

3.1 Synthesis and characterisation

Scheme 1: Synthetic procedure followed for the synthesis of complexes 1-5

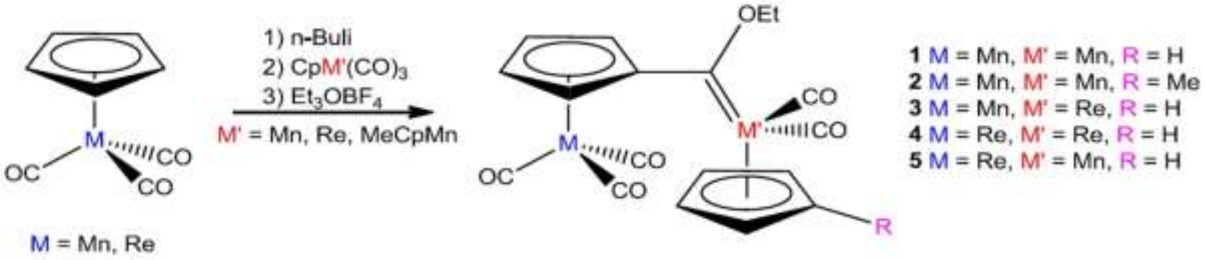

Complexes **1-5** were synthesised as major products in the reactions based on classic Fischer methodology (Scheme 1) [26]. During the synthesis of complexes **2** and **3**, the formation of the homonuclear bimetallic monocarbene complex **1** [10] was observed as a minor side product and isolated in low yields [10]. The bimetallic-CpRe monocarbene complex, **4**, was also isolated as a side product in the synthesis of **5**. The infrared (IR) spectrum of **1** has been reported [10] and the spectra of **2-5**, using hexane as the solvent, showed the presence of four stretching frequencies. The IR spectra of **1-5** indicate two stretching frequencies attributed to the tricarbonyl moieties and two observed frequencies attributed to the carbene metal carbonyl stretching frequencies. Two stretching frequencies for both the $Re(CO)_2$ and the $Mn(CO)_2$ moiety were observed between 1889 and 1952 cm^{-1} and stretchings were seen in the same region regardless of the identity of the metal centre. The observation of these stretching frequencies are supported by literature [13,14]. NMR spectroscopy indicates downfield-shifted carbene carbon peaks between $\delta = 269.1$ and 331.3 ppm. The carbene peaks were also significantly more deshielded for the complexes where the carbene carbon were coordinated to a $Mn(CO)_2$ moiety compared to the rhenium analogue. These structural characterisations were also confirmed with X-ray diffraction studies of the three complexes and will be presented in the next section.

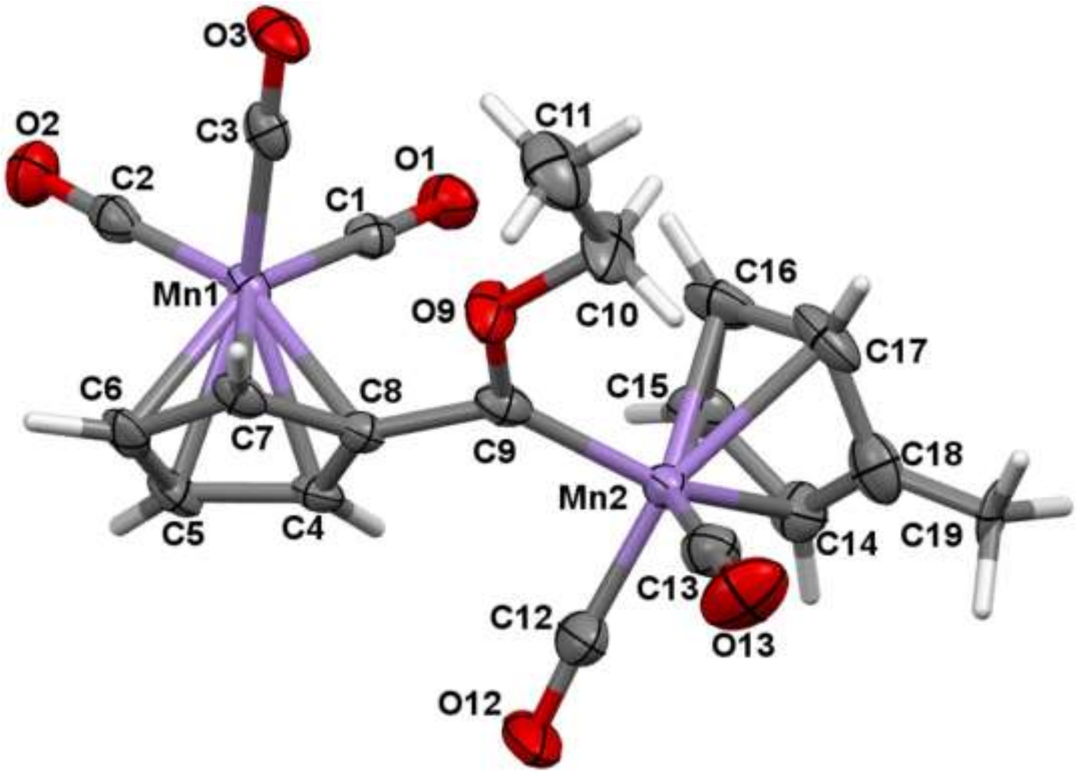

Figure 7: Perspective view of 2 with thermal ellipsoids drawn at the 50% probability level

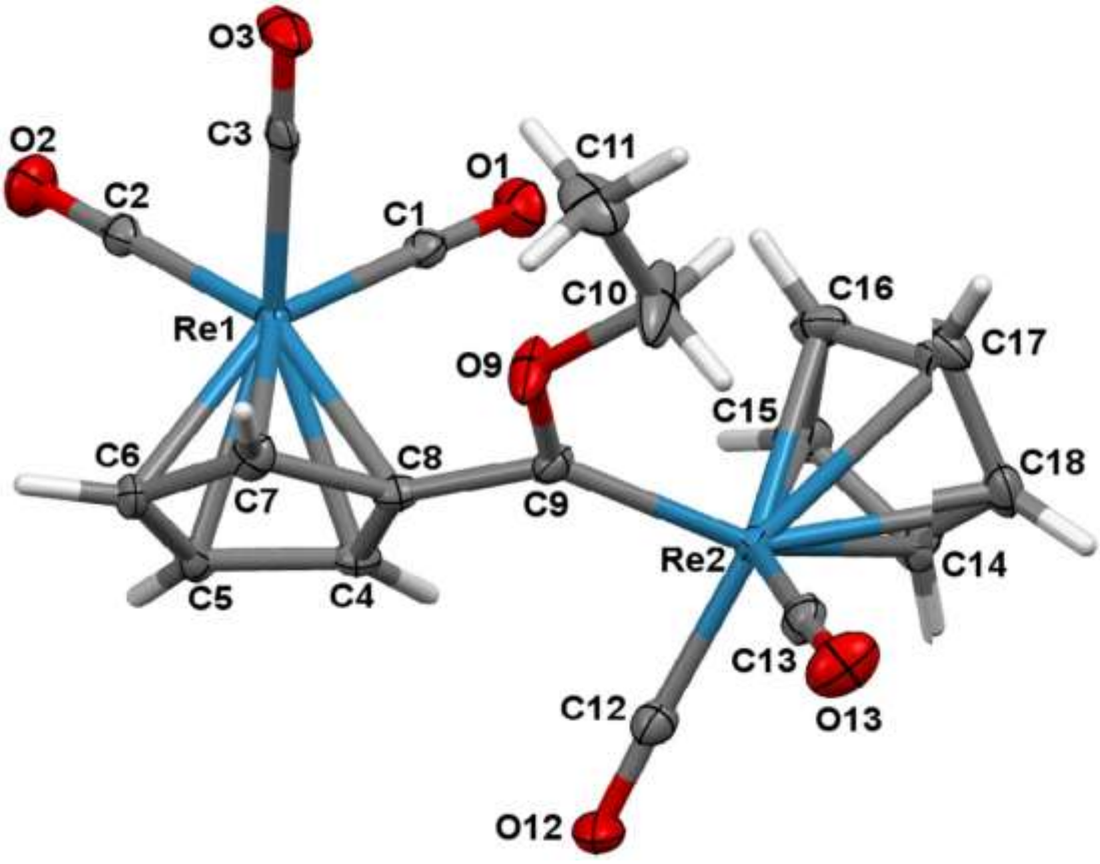

Figure 8: Perspective view of 4 with thermal ellipsoids drawn at the 50% probability level

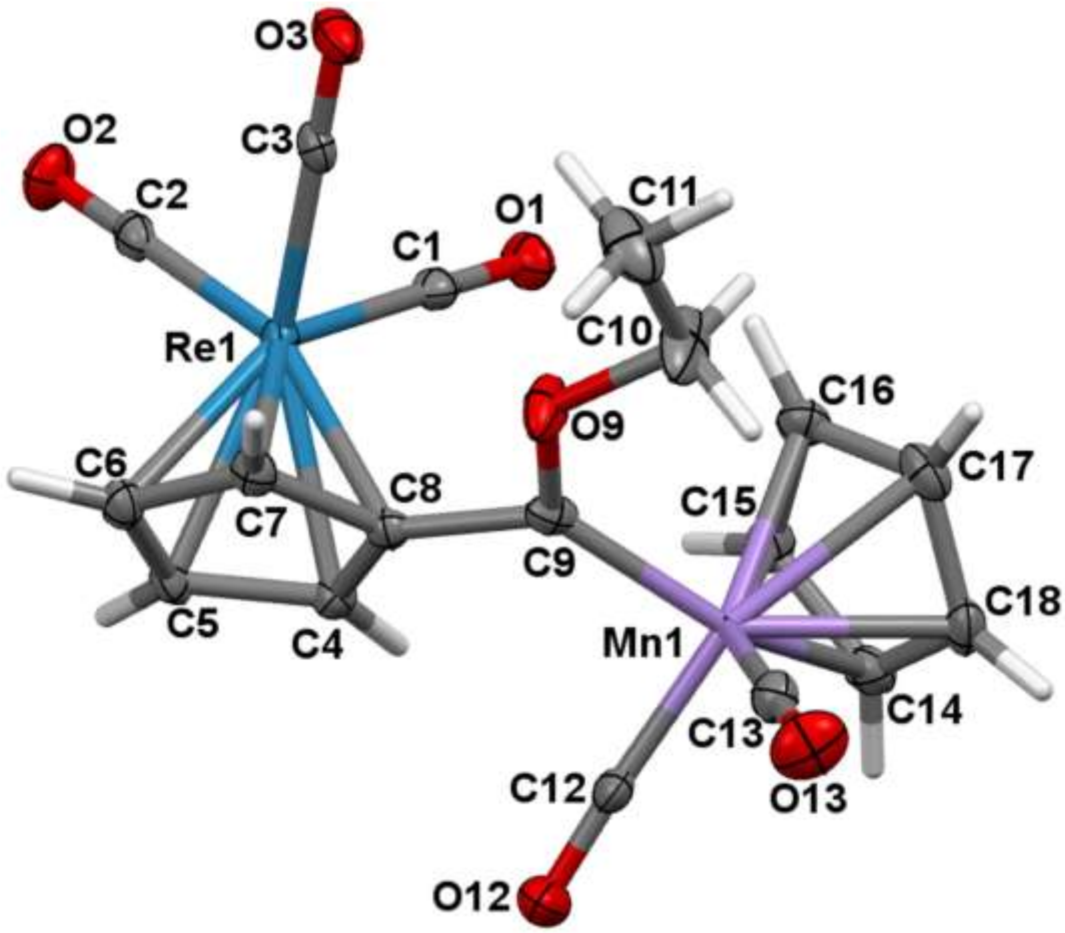

Figure 9: Perspective view of 5 with thermal ellipsoids drawn at the 50% probability level

The three molecular structures, complex **2**, **4** and **5** were isostructural. In addition, complex **2** could not be separated successfully from the mixture of complexes **1** and **2**, and this resulted in the co-crystallisation of complex **1** and **2** in a 0.69465: 0.30535 ratio. Selected structural parameters of importance are summarized in Table 1. The carbene ligand, as defined by the C10-O9-C9-M'dihedral angle, deviates from planarity by less than 9° in all three complexes. The carbene-metal bond distance was found to be 1.919(6), 2.022(5) and 1.918(6) for **2**, **4** and **5** respectively and indicated limited deviation between the manganese and rhenium carbene complex when cyclopentadienyl rhenium tricarbonyl serves as starting synthon. The bond distances reflect the double bond character of M'=C9. These values are similar to the M=C bond for analogous complexes with heteroarene substituents instead of a cyclopentadienyl metal substituent. The angles between the carbene plane (M'-C9-O9 and C8) and the plane of the Cp ring (C14 - C18) are very similar for complexes **2**, **4** and **5** (*ca.* 37°). Of significance is the orientation of the cyclopentadienyl metal moieties towards one another (preference of the *trans*-orientation) indicating possible interactions between the groups on the carbene ligand and the carbonyl groups of the metal associated with the carbene moiety. These interactions will further be described in the DFT study section. The angle between the planes defined by the Cp ligands were determined to be similar for complexes **2**, **4** and **5** (*ca*. 47°).

Table 1. Selected bond lengths and angles for 2, 4, and 5.

	2	**4**	**5**
Bond length (Å)			
M–COx (*x* = 1–3)	1.796(6)	1.912(5)	1.916(5)
M′–C9	1.919(6)	2.022(5)	1.918(6)
C8–C9	1.485(7)	1.483(6)	1.489(7)
O9–C9	1.336(6)	1.333(5)	1.336(7)
M′–COx (*x* = 12, 13)[a]	1.767(7)	1.893(5)	1.775(6)
Bond angle (°)			
O9–C9–M′	129.1(4)	126.8(3)	129.0(4)
C8–C9–M′	121.2(3)	126.8(3)	126.6(4)
O9–C9–C8	103.9(7)	104.4(4)	104.4(4)
Torsion angle (°)			
C10–O9–C9–M′	6.0(8)	4.1(8)	8.6(9)
C7–C8–C9–M′	164.5(4)	168.6(4)	165.2(4)
C4–C8–C9–M′	−19.7(8)	−13.8(7)	−17.5(8)
Plane angle (°)			
Carbene/Cp	37.59	36.58	36.60
Cp/Cp	47.59	4.88	46.74

[a] Average value for metal-carbonyls

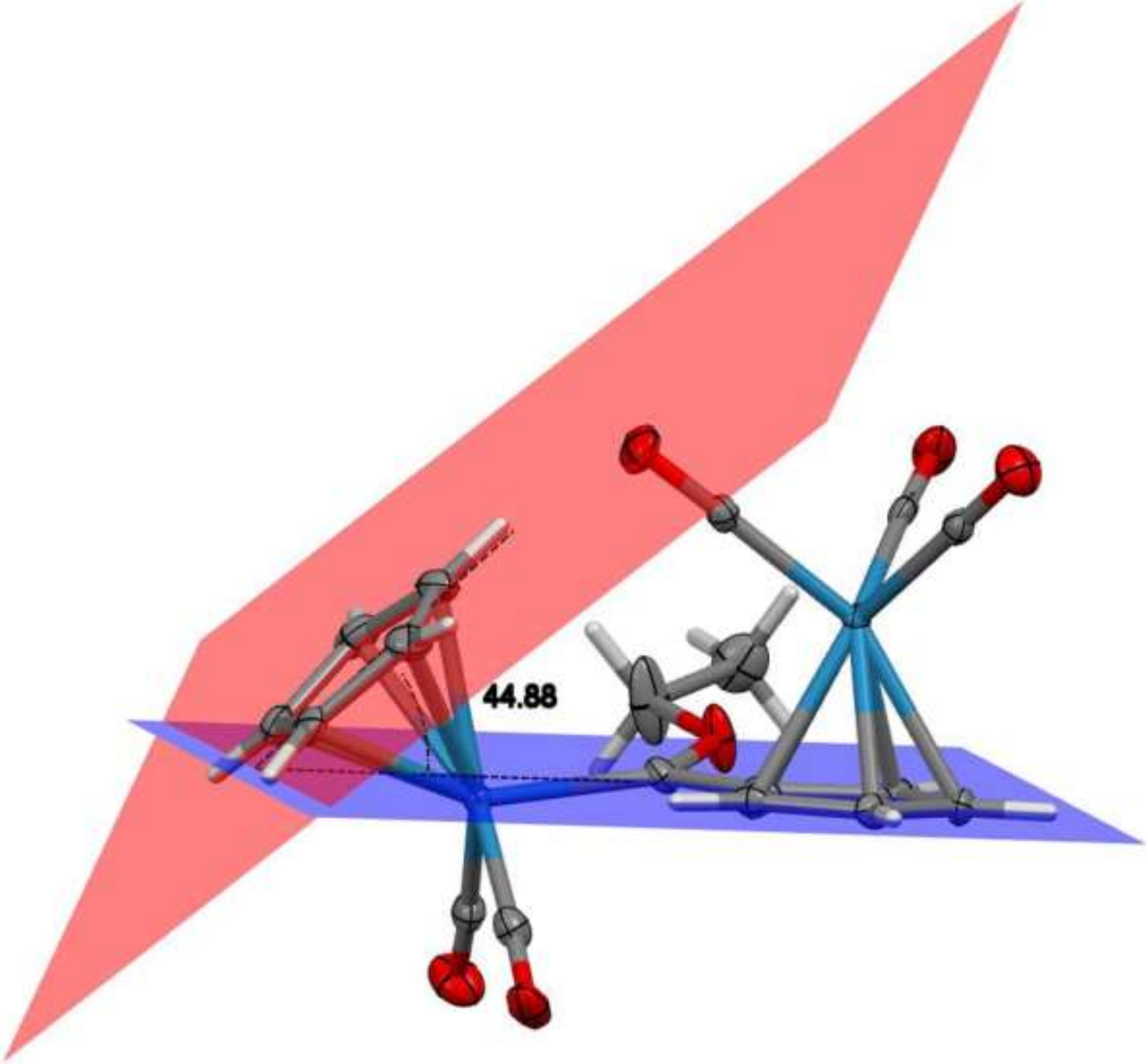

Figure 10: Plane angle between the two Cp ligands of the dirhenium complex 4.

The plane angles between the two Cp ligands in reference to one another have been determined for the *cis*- and vertical coordination mode conformers and were established to be 21.67º and 44.79º respectively. The angle between the carbene ligand and the metallating metal Cp was found to be 47.33º for the *cis* conformer and 79.23º for the vertical coordination mode.

3.3 DFT study

A DFT study was undertaken to investigate certain aspects of the dinuclear carbene species. Firstly, the rotational conformation preferred by the carbene metal cyclopentadienyl moiety in reference to the metal cyclopentadienyl starting synthon will be calculated and secondly, an investigation into which synthetic step determines the resulting *cis* or *trans* conformation of the final product will be determined. Finally experimental carbene bond lengths were compared to theoretically generated carbene bond lengths as a simple indication as to the validity of the applied model. In this study, Wiberg bond indices were calculated to provide theoretical support for the determination of rotation barriers within the molecule. The dinuclear carbene complexes have two possible conformations in the solid state, namely the *cis* or *trans* conformations of the cyclopentadienyl ring of the cymantrenyl substituent relative to that of the carbene metal moiety (Figure 5). Gas-phase theoretical calculation results show that the energies of *cis* and *trans* conformations of the Cp rings relative to one another are comparable (Table 2); however, the *trans* conformation remains lower in energy for complexes **1**-**5** (Figure 11), supporting the conformation determined in the solid-state structure (Figures 7-9). The energy of the horizontal coordination mode has been determined to be lower for all the complexes in this study compared to the vertical mode as described by Lugan [11] and Hoffman [12].

Table 2: Calculated energy values of the *cis* and *trans* conformations for 1–5..

Complex	***Cis* (kJ mol^{-1})**	***Trans* (kJ mol^{-1})**	**Vertical mode (kJ mol^{-1})**	**Horizontal mode (kJ mol^{-1})**
1	+1.2	0	+7.3	0
2	+1.2	0	+7.7	0
3	+1.3	0	+2.0	0
4	+4.3	0	+1.2	0
5	+3.3	0	+9.4	0

Minor energy difference between the two conformations permits both conformations to be experimentally feasible. The incidence of the methoxy analogue of **4** provides an example of a solid state structure of a *cis*-orientated carbene complex [$C_5H_5Re(CO)_2\{C(OMe)C_5H_4Re(CO)_3$] [14]. However, the solid state structures of the ethoxy complexes (**1**, **2**, **4**, **5**) all exhibit the *trans* orientation.

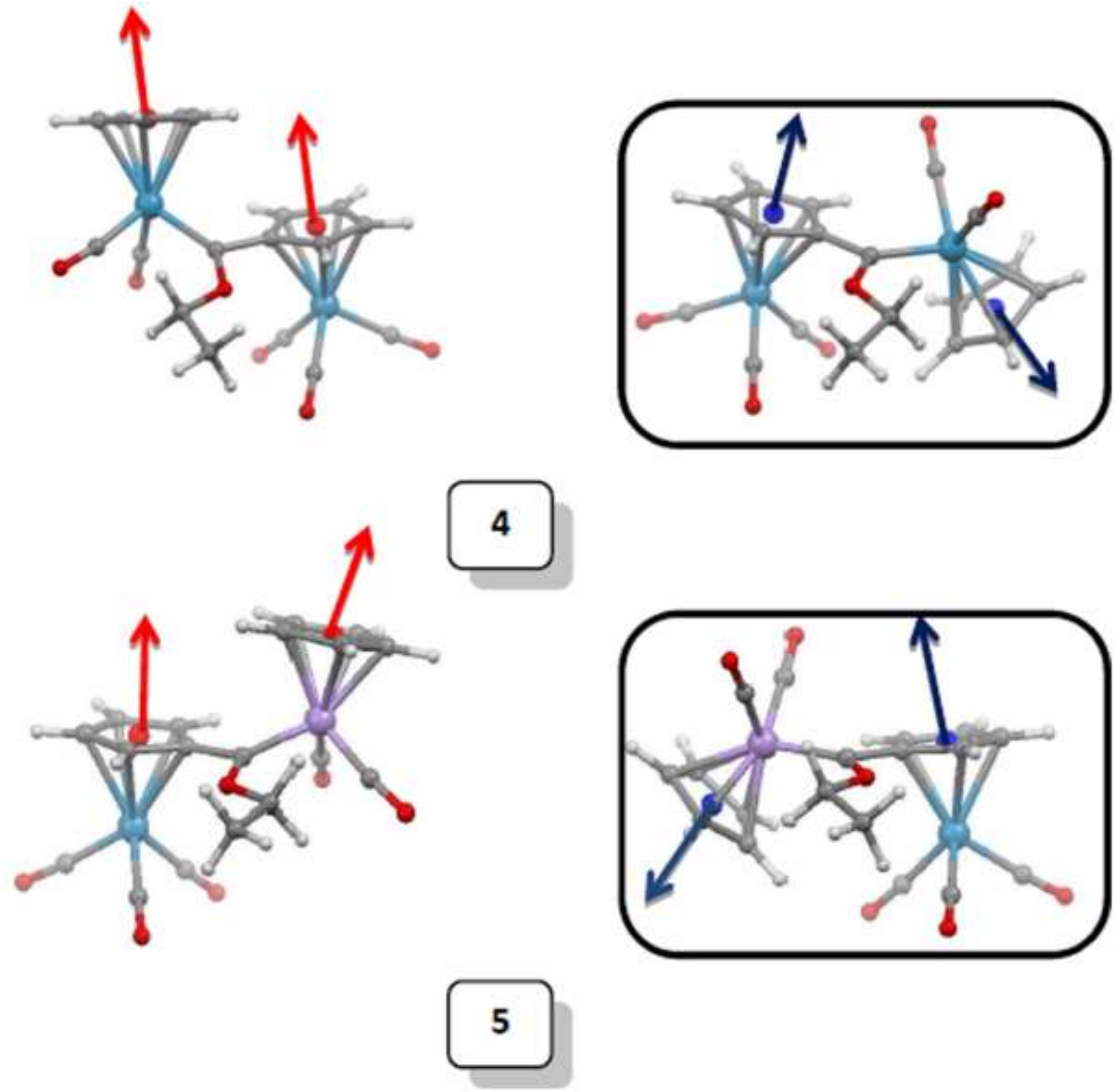

Figure 11: Optimized *cis* (left) and *trans* (right) conformations for 4 and 5

Numerous intermolecular close contact interactions observed in the packing of the carbene complexes in favour of the *trans*-conformation, can be witnessed. A few of these interactions are shown in Figure 12 and these interactions range from 2.499 to 2.694Å.

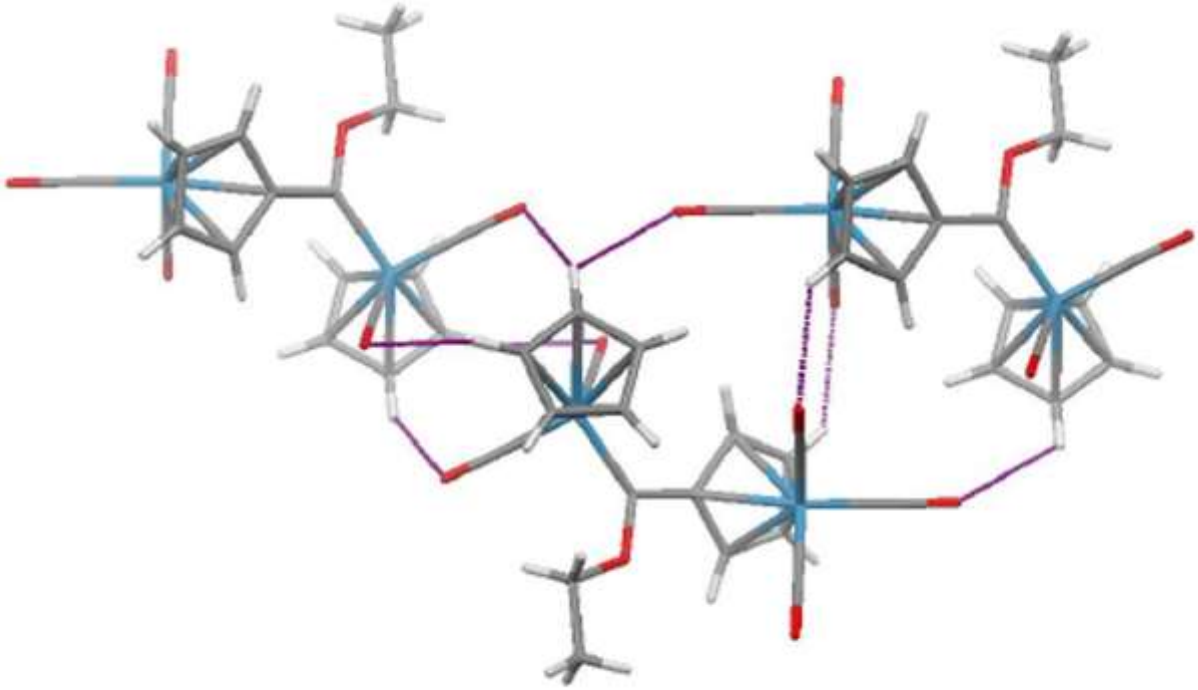

Figure 12: Intermolecular close contact interactions in the crystal packing of 4

The formation of the metal acylate should establish delocalization of electron density from the acylate to the carbene metal moiety (Figure 13) [27]. The delocalized system provides extra electron density to the highly electrophilic carbene centre. Donation from the other alkyl or aryl substituent is only feasible in situations where the substituent contains additional donating groups such as hydroxyl or alkoxy groups. Rotation around the metal-carbene bond and metal-oxygen acylate bond should thus be restricted (Figure 13). Taking the theoretical bond orders into consideration, significant π-contribution from the ethoxy to the carbene carbon is witnessed with the greatest double bond character seen between the carbene carbon and alkoxy substituent (Table 3). Wiberg bond indices have found application in determining the bond order in carbene complexes [28] and seem to indicate that the bond between the carbene carbon and the carbene metal displays almost exclusively σ-bond character, or that in the case where π-contribution is present, that this contribution was found to be almost negligible.

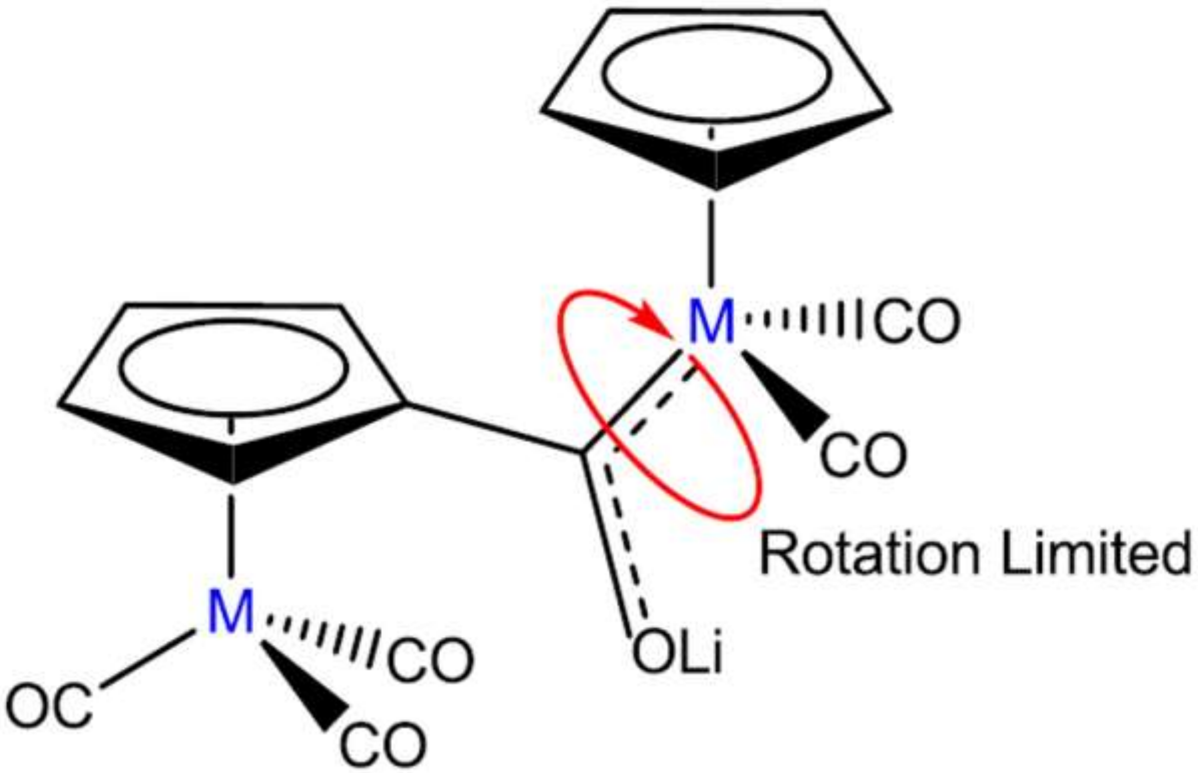

Figure 13: The delocalized electronic system after the formation of the metal acylate

Although literature provides sound precedence defining the carbene moiety as an σ-donating π-accepting ligand, our calculations indicate that the π-donation from the ethoxy substituent to the carbene centre takes preference above the π-donation from the metal species. This finding also correlates with literature reports by Fischer *et al.* [29]. The bond order between the carbene and oxygen acylate substituent also diminishes after alkylation, with limited variation between the metal-carbene bond and between the carbene and the cyclopentadienyl metal substituent. The bond order slightly increases between the carbene metal and the carbene carbon upon alkylation of the acylate. The formation of a six-membered metal acylate ring affords ridged stability within the molecule (Figure 14) and also restricts rotation around the metal-carbon double bond.

Slightly higher bond orders are calculated when the $CpRe(CO)_3$ acts as the metallating agent, which is expected since the carbene metal, possessing of a greater electon density, would be able to contribute this density towards the electrophillic carbene carbon. This electronic aspect is also mirrored by the slightly lowered bond order between the carbene carbon and the ethoxy carbene. Total bond indices are calculated for the carbene carbon atom and indicate non-ideal values of below 3.5 (ideal BO = 4) and indicate the limitation of this method for accurately calculate bond orders.

Table 3: Wiberg bond indices for the carbene complexes 1-5 and acylates

Complex	**Wiberg bond indices**			
	C_{carb}–M	**C_{carb}–O**	**C_{carb}–C_{Cp}**	**Total**
1	0.99	1.17	1.09	3.25
2	0.97	1.17	1.10	3.24
3	1.09	1.11	1.09	3.29
4	1.10	1.12	1.08	3.30
5	0.98	1.18	1.09	3.25
Cis Li-acylate	0.92	1.48	1.02	3.42
Trans Li-acylate	0.92	1.46	1.02	3.40

Based on bond orders of above 1, rotation around the carbene carbon and the cyclopentadienyl metal substituent should still be possible. As supported by literature [29], the calculated bond orders indicate limited or no π-contribution from this substituent. The formation and prevalence of the *trans* carbene complex could thus only be attributed to either the energetics of the formed product or additional stabilization within the molecule after formation. An NBO analysis of the carbene complexes found internal stabilization between the ethoxy substituent and the carbene metal carbonyl moieties and favours the formation of the *trans* conformer.

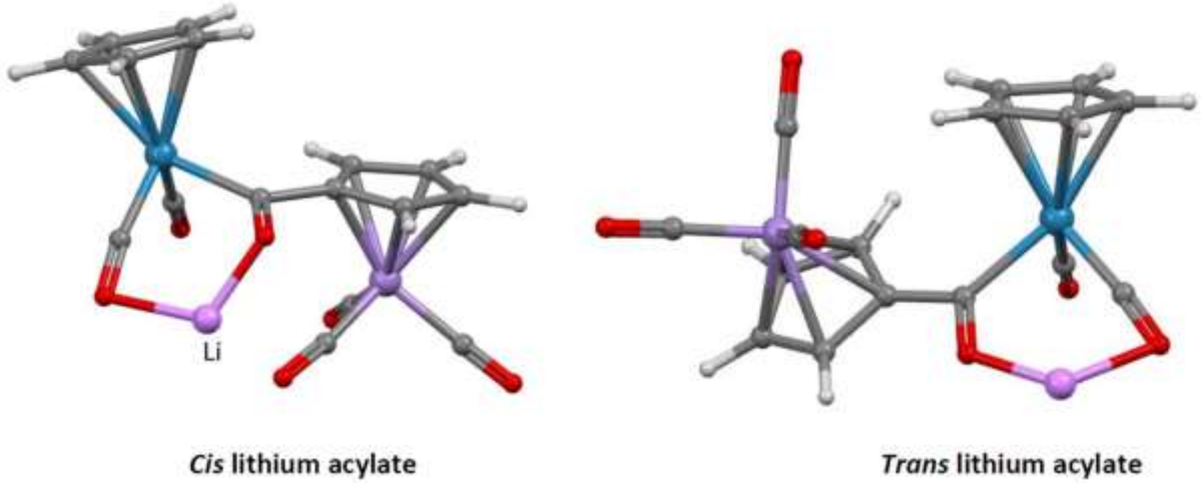

Figure 14: Stabilization through a six-membered acylate ring for complex 3

Incidences of non-covalent intramolecular ligand interactions are witnessed between the methylene protons of the carbene substituent and the metal carbonyl ligands associated with the carbene moiety. Interaction energies determined between 2.1 and 2.9 kJ/mol were observed for **1**-**5**. The interactions, although weak, were completely absent in the *cis* conformations and could contribute to the stability and preferential formation of the *trans* conformer (Figure 15).

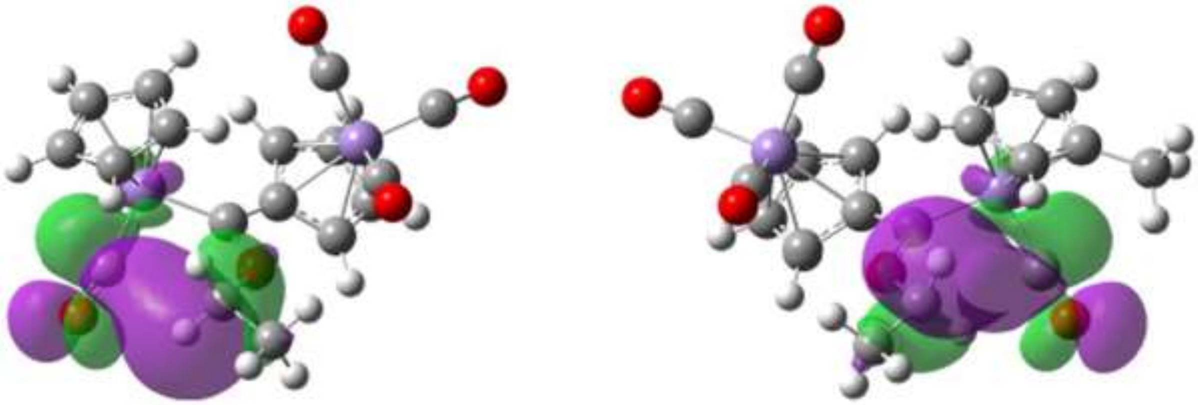

Complex 1: 2.93 kJ/mol

Complex 2: 2.34 kJ/mol

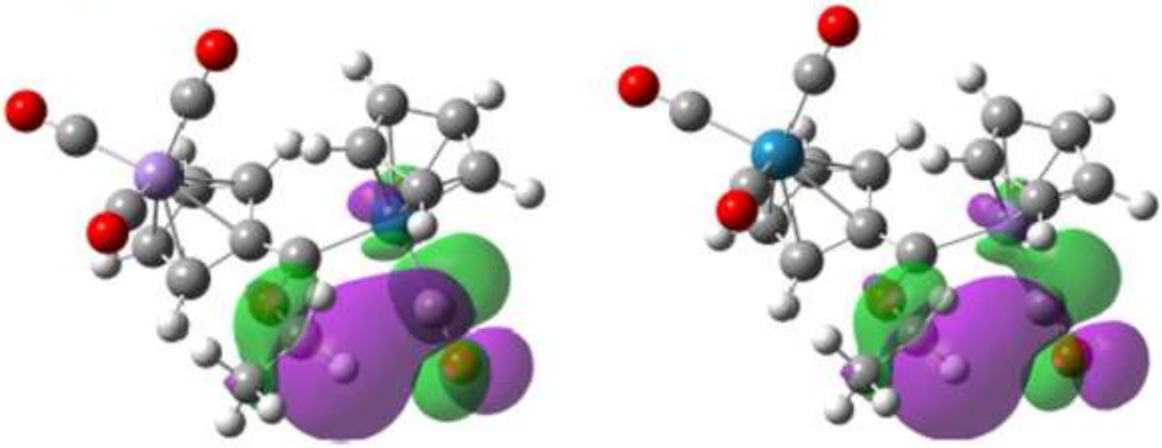

Complex 3: 2.64 kJ/mol

Complex 5: 2.13 kJ/mol

Figure 15: NBO interactions in the *trans* conformation

In contrast with the published values of Lugan et al. [11], theoretical results for the complexes of this study show no stabilization from the π-(C≡O) orbital of a carbonyl ligand on the carbene metal moiety [Mn] or [Re] to the unoccupied σ*-($C-H_{OEt}$) orbital in **1**-**5**. Only σ-($C-H_{OEt}$) → π*-(C≡O) interactions were observed between OEt and CO ligands of the carbene metal moiety and these interaction values are less significant than the values reported by Lugan *et al.* [11]. This may be due to the difference in horizontal (our complexes) and vertical (Lugan *et al.*) orientations of the carbene substituents. To provide insight into the energetics of the carbene formation, and in regards to the prevalence of the *trans* conformation, a full energy profile of the carbene synthesis has been calculated (Scheme 2). Lithiation of the cyclopentadienyl metal synthon leads to the formation of the lithiated cyclopentadienyl metal species, with a sharp decrease in the energy of the molecule. The energy release is accompanied by the formation of the very stable butane and the lithium entity, now stabilized by the larger $CpMn(CO)_3$ moiety. The formation of the $LiCpMn(CO)_3$ is achieved by the irreversible deprotonation through the employment of a strong base such as n-butyl lithium. The formation of the metal acylate is accompanied by the release of energy to produce a more stable intermediate and the *cis* conformation, surprisingly, exhibits higher stability compared to the *trans* conformer. The final carbene complex favours the formation of the *trans* conformer, regardless of the identity of the starting metal synthon or the metalating agent. The *trans* complex is more favourable when $CpRe(CO)_3$ acts as the deprotonated moiety compared to $CpMn(CO)_3$ and in addition, the *trans* complex is also favoured when $CpRe(CO)_3$ acts as the metalating agent. From Table 2, the *trans* complex of **4** would thus be the most preferential, consisting only out of $CpRe(CO)_x$ fragments and will be followed in stability by **5**, which is a *trans* carbene complexes where $CpRe(CO)_3$ served only as the initial deprotonated synthon. Since we are interested in the nature of the conformation around the carbene-metal moiety, the correlation between experimental results and theoretical findings plays a crucial role in the validation of the computation results. An analysis was undertaken to correlate the structural properties of the M-carbene fragment to that of theoretical findings and a plot of calculated verses experimental M-carbene bond lengths is displayed in supplementary data. The data displays a satisfying linear relationship, with the regression line having a R^2 value of 0.99. The theoretical carbene-metal bond length is also 0.011 pm longer on average compared to the experimentally determined structural parameter.

Scheme 2: Energy plot for the synthetic methodology that was followed in the formation of the *cis* (red) and *trans* (blue) product.

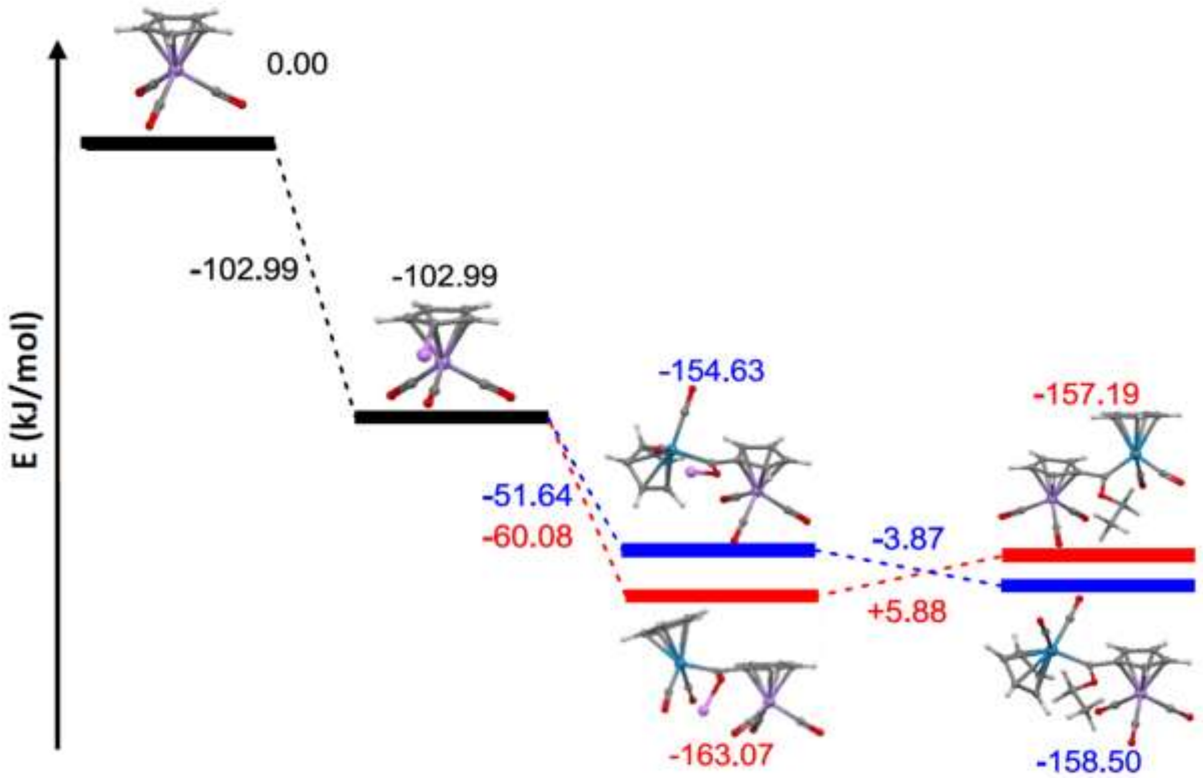

As mentioned previously, the theoretical lithium acylate intermediate shows an interaction between the lithium counter ion and one of the carbonyl ligands of the carbene metal. The formation of the six-membered ring influences the binding structure of the lithium acylate considerably and stabilization of the positive ion with the carbonyl ligands occurs preferentially towards the carbene centre carbonyls compared to that of the substituent half-sandwich metal synthon. The interaction can easily be explained when the electrostatic potential maps of the acylates are taken into consideration (Figure 16). The ESP map indicates the presence of highly negative carbonyl groups of the carbene centre especially in comparison to the substituent CpM(CO)$_3$ carbonyl groups. The carbene carbonyl group, stabilized by the lithium ion, has more equally shared electron density over the entire ligand group compared to the non-stabilized carbonyl ligand. Re-C and C-O bond orders were determined as 1.59 and 1.74 respectively for the stabilized-ligand compared to 1.37 and 1.99 for the non-stabilized carbonyl group in the *cis* conformer. The *trans* conformer indicated an even greater sharing of electron densities and the bond orders of the Re-C and C-O bonds, of the stabilized carbonyl ligand, were calculated as 1.66 and 1.71 respectively. The bond orders of the non-stabilized carbonyl ligand were determined as 1.32 and 2.02 for the Re-C and C-O bonds respectively.

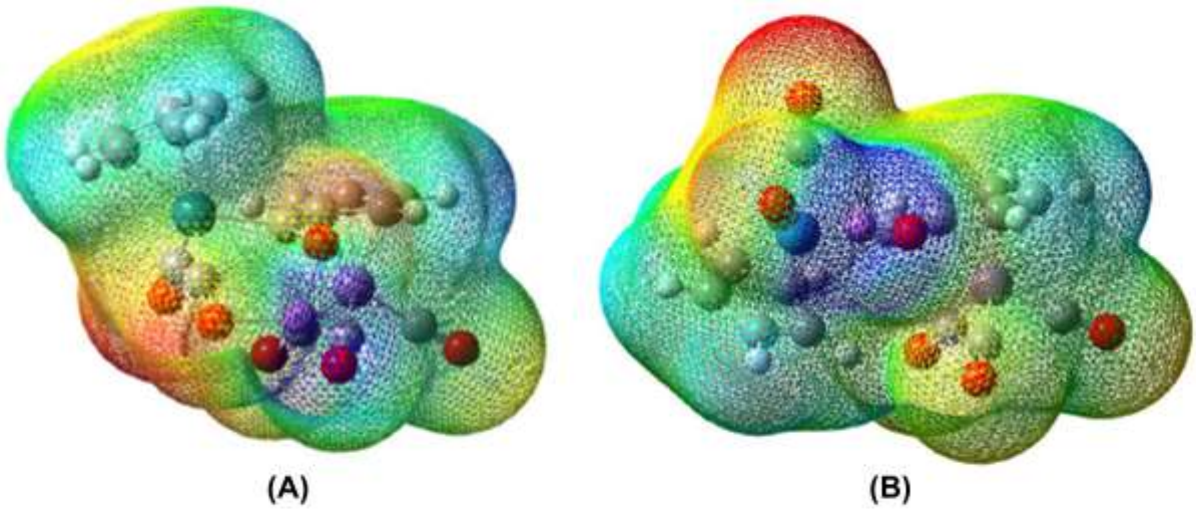

Figure 16: Electron potential map of the *cis*-acylate (a) and the *trans*-acylate (b) of 3

4 Conclusion

Bimetallic complexes **2-5** were synthesized in satisfactory yield. The molecular structures of the novel complexes were confirmed with NMR and IR spectroscopy, and single crystal X-ray diffraction studies of **2** and **4** and **5**. Applying DFT calculations, it was possible to explain and visualise conformational stabilities of the *cis* and *trans* conformers as well as to determine the origin of the preferential conformation by means of an energy plot. Complexes **1-6** were found to be more stable in the *trans* conformation compared to this *cis* conformer. The preference of the *trans* conformers above the *cis* analogues are also witnessed in the solid state structure. Theoretical calculations indicated the origin of stabilization of the electrophilic carbene centre through greater π-donation from the ethoxy substituent and less back donation from the carbene metal moiety towards the carbene carbon atom. NBO stabilization interactions were visualized and illustrated the ability of the *trans* conformer to produce intramolecular stabilization between the methylene protons of the ethoxy substituent and the carbonyl ligands associated with the carbene metal moiety. These interactions were absent in the *cis* conformation. The calculated results of the lithium acylate intermediate suggest internal stabilization via the formation of a six-membered ring. Theoretical calculations were validated by a comparison between experimental and calculated carbene-metal bonds. The results provide an indication as to the steric and electronic parameters governing the conformations of the dimetallic carbonyl complexes.

Acknowledgements

This work has received financial support from the South African National Research Foundation (Grant nr. 93638) and the University of Pretoria. The authors wish to thank Prof J. Conradie and Dr M.M. Conradie, University of the Free State, as well as Mr D.C. Liles, University of Pretoria, for their valuable input.

References

---

[1] E.O. Fischer, A. Maasböl. *Angew. Chem. Int. Ed. Engl.*, **580**, 3 (1964).

[2] A. de Meijer, H. Schirmer, M. Duetsch. *Angew. Chem. Int. Ed.*, **39**, 3964 (2000).

[3] J. Barluenga. *J. Pure Appl. Chem.*, **68**, 543 (1996).

[4] J. Barluenga, J. Santamaría, M. Tomás. *Chem. Rev.*, **104**, 2259 (2004).

[5] M. A. Sierra. *J. Am. Chem. Soc.*, **123**, 851 (2001).

[6] K. H. Dötz. *Angew. Chem.*, **87**, 672 (1975).

[7] E. O. Fische, F. J. Gammel, J. O. Besenhard, A. Frank, D. Neugebauer. *J. Organomet. Chem.*, **191**, 261 (1980).

[8] J. G. López-Cortés, L. F. C. de la Cruz, M. C. Ortega-Alfaro, R. A. Toscano, C. Alvarez-Toledano, H. Rudler. *J. Organomet. Chem.*, **690**, 2229 (2005).

[9] U. Behrendt, R. M. Pfeifer, R. Wartchow, H. Butenschön. New J. Chem., 23, C73 (1982).

[10] R. Fraser, P.H van Rooyen, M. Landman. *J. Mol. Struct.*, **1105**, 178 (2016).

[11] N. Lugan, I. Fernández, R. Brousses, D. A. Valyaev, G. Lavigne, N. A. Ustynyuk. *Dalton Trans*., **42**, 898 (2013).

[12] B. E. R. Schilling, R. Hoffmann, D. L. Lichtenberger. *J. Am. Chem. Soc*., **101**, 585 (1979).

[13] E.O. Fischer, V.N. Postnov, F.R Kreissl. *J. Organomet. Chem*., **231**, C73(1982).

[14] C.P. Casey, C.J. Czerwinski, R.K. Hayashi. *Organometallics,* **15**, 4362(1996).

[15] D.F. Schriver, M.A. Drezdzon. *The manipulation of Air-Sensitive Compounds, 2nd ed.,* Wiley, New York, USA, (1986).

[16] H. Meerwein. *Org. Synth.*, **46**, 113(1966).

[17] APEX2 (including SAINT and SADABS); Bruker AXS Inc., Madison, WI (2012).

[18] G.M. Sheldrick. Acta Crystallogr., **A64**, 112 (2008).

[19] L.J. Farrugia. *J. Appl. Crystallogr*., **30**, 565(1997).

[20] M.J. Frisch, G.W. Trucks, H.B. Schlegel, G.E. Scuseria, M.A. Robb, J.R. Cheeseman, G. Scalmani, V. Barone, B. Mennucci, G.A. Petersson, H. Nakatsuji, M. Caricato, X. Li, H.P. Hratchian, A.F. Izmaylov, J. Bloino, G. Zheng, J.L. Sonnenberg, M. Hada, M. Ehara, K. Toyota, R. Fukuda, J. Hasegawa, M. Ishida, T. Nakajima, Y. Honda, O. Kitao, H. Nakai, T. Vreven, J.A. Montgomery (Jr), J.E. Peralta, F. Ogliaro, M. Bearpark, J.J. Heyd, E. Brothers, K.N. Kudin, V.N. Staroverov, T. Keith, R. Kobayashi, J. Normand, K. Raghavachari, A. Rendell, J.C. Burant, S.S. Iyengar, J. Tomasi, M. Cossi, N. Rega, J.M. Millam, M. Klene, J.E. Knox, J.B. Cross, V. Bakken, C. Adamo, J. Jaramillo, R. Gomperts, R.E. Stratmann, O. Yazyev, A.J. Austin, R. Cammi, C. Pomelli, J.W. Ochterski, R.L. Martin, K. Morokuma,

V.G. Zakrzewski, G.A. Voth, P. Salvador, J.J. Dannenberg, S. Dapprich, A.D. Daniels, O. Farkas, J.B. Foresman, J.V. Ortiz, J. Cioslowski, D.J. Fox, Gaussian 09, Revision D.01, Gaussian Inc., Wallingford CT, (2010).

[21] A.D. Becke. *J. Chem. Phys.*, **98**, 5648 (1993).

[22] C. Lee, W. Yang, R.G. Parr. *Phys. Rev*., **B 37**, 785(1988).

[23] F. Weigend, R. Ahlrichs. *Chem. Phys.*, **7**, 3297(2005).

[24] J.W. McIver, A.K. Komornicki. *J. Am. Chem. Soc.*, **94**, 2625 (1972).

[25] (a) J.P. Foster, F. Weinhold. *J. Am. Chem. Soc*., **102**, 7211(1980); (b) A.E. Reed, F. Weinhold. *J. Chem. Phys.*, **83**, 1736 (1985); (c) A.E. Reed, R.B. Weinstock, F. Weinhold. *J. Chem. Phys.*, **83**, 735 (1985); (d) A.E. Reed, L.A. Curtiss, F. Weinhold. *Chem. Rev*., **88**, 899 (1988).

[26] See Ref. [5] and references therein.

[27] J. A. Connor, E. M. Jones. *J. Chem. Soc.*, 1974 (1971).

[28] G. Occhipinti, H. R. Bjørsvik, K. W. Törnroos, A. Fürstner, V. R. Jensen. *Organometallics*, **26**, 4383 (2007).

[29] E. O. Fischer. *Pure Appl. Chem.*, **30**, 353 (1972).